DYNAMIC SYSTEM COMPOSED OF TOPDRIVE AND DRILL PIPE

SISTEM DINAMIC COMPUS DIN TIPDRIVE ȘI GARNITURĂ DE FORAJ

Marius STAN[1], Niculae Napoleon ANTONESCU[2],
Costin Viorel VLĂȘCEANU[3], Ammar MULLA[4]

Abstract: *To emphasize the extent to which theoretical research results are consistent with the real phenomenon it is necessary to carry out an experimental study. It has been the design and implementation of an unconventional model of drilling equipment designated to simulate digging wells and it is provided and structure driving to unconventional maneuver system. The model is similar to the drilling rig for unconventional drilling. The choice was not random, because there were concerns about research and design of a similar installation in the design institute and UPG Ploiesti, the unfinished project model was not verified yet. To verify some of similarity must be some acceptable degree of geometric similarity, kinematic and dynamic with the real unconventional rig used at UPG Ploiesti.*

Keywords: design, method, drilling, structure, theory.

Rezumat: *Pentru a sublinia măsura în care rezultatele cercetării teoretice sunt în concordanță cu fenomenul real este necesar să se efectueze un studiu experimental. A fost proiectat și realizat un model neconvențional de echipament de foraj destinat să simuleze săparea sondelo cu diametru mare. Modelul este similar cu instalația de foraj pentru foraj neconvențional. Alegerea nu a fost întâmplătoare, deoarece au existat preocupări cu privire la cercetarea și proiectarea unei instalații similare în institute de proiectare și UPG Ploiești, modelul de proiect nefinalizat încă de către acestea nu a fost verificat. Pentru a verifica unele similarități trebuie să existe un grad acceptabil de similitudine geometrică, cinematică și dinamică cu platforma neconvențională reală, utilizat in cadrul UPG Ploiesti.*

Cuvinte cheie: proiectare, metodă, foraj, structură, teorie.

[1] Associate Prof Ph.D. Eng.., Dept. of Mechanical Engineering, Petroleum and Gas University of Ploiesti, Romania, e-mail: mstan@upg-ploiesti.ro
[2] Prof. Ph.D. Eng., Dept. of Mechanical Engineering, Petroleum and Gas University of Ploiesti, Romania, e-mail: nnantonescu@upg-ploiesti.ro
[3] Lecturer Ph.D. Eng., Dept. of Petroleum Geology and Reservoir Engineering, Petroleum and Gas University of Ploiesti, Romania, e-mail: viorel.vlasceanu@upg-ploiesti.ro
[4] Ph.D. Student Eng., Dept. of Mechanical Engineering, Petroleum and Gas University of Ploiesti, Romania, e-mail:

1. Introduction

Drilling rigs for large diameter wells (IFDM), hydraulic case best reflects the actual behavior and unconventional evolution of work systems. In the U.S., Hughes Tool Co. Company [7]. Special hydraulic systems are built with small dimensions and high power. In our country, in I.P.C.U.P. Ploiesti [8], was designed a hydraulic installation of this type (PF 900), for drilling large-diameter wells. What is common to these types of drilling rigs is the super structure of the plant and its functionality [1],[3].

Resistant structure (SG) is U-shaped back, called reactive guidance and structure (SGR) because it takes time given the task of overturning. It represents the support for the suspended drill string during drilling operations to handle the whole bottom. Device for suspension of the drilling string is called the mobile platform (PM), as it moves along with the four vertical hydraulic cylinders which is secured by running the drilling handle on all gaskets [8],[2].

The entire load is taken through the mobile platform PM the hydraulic cylinder rods. The mobile platform is the most requested item of construction because it takes both effort and pregnancy the end of the race due to the desync Movement of hydraulic cylinders. The structure provides only reactive directions guiding the effect of wind motion-taking efforts, desync, mounting errors, and their weight. Overall, the actual installation is mounted on a sub-resistant metal or the ground on a concrete foundation.

As the design of the machine 900 can perform hole PF diameter of 6.0 m (20 ft) and depths exceeding 600 m. SG or SGR, four feet of the pipe has a height of 12 m and is designed to give stability and rigidity to the assembly that guides PM. Hydraulic cylinders are designed to raise together a full load F = 9 MN. The maneuver can develop speeds of up to 0.16 m/s at entry and 0.08 m/s at the drawing [5].

2. The principles of stand design for unconventional drilling facilities

This is done by similarity theory, which allows analysis and synthesis of small-scale experimental phenomena. To this end, the building-reduced model (stand) is identified with the attempt to develop a sepsis who meets the criteria of similarity between the sizes of the same kind of physical. Research methods and processes of natural phenomena can be theoretical and experimental [6].

Theoretical methods consisted of applying the fundamental laws of physics and mathematical devices to study the phenomenon. The experimental method is proposed to perform the actual physical phenomena and will study their reproduction in the laboratory. The construction of the sepsis, which ultimately is the booth, was considered geometric similarity, similarity in mass distribution, kinematic similarity, and dynamic similarity[14].

Geometric similarity: the corresponding points located on the same phenomena sepsis and prototype are geometrically similar; kinematic similarity-the points corresponding speeds and trajectories are also proportional; dynamical similarity-the same type of forces corresponding points are proportional [11].

For the two physical phenomena, having the same class, to be similar, it is necessary and sufficient that their adequate similitude criteria to be equal, and the oneness conditions to proportional. For example, if the chosen measurements are unit 1 (m_1), unit 2 (m_2), and unit 3 (m_3), by applying the theorem, it results[10], [3]:

$$[L]^0 [M]^0 [T]^0 = [m_1]^{\alpha} [m_2]^{\beta} [m_3]^{\gamma} \cdot \{ [L]^a [M]^b [T]^c \}^{\delta} \qquad (2.1)$$

From the previous chapters, important physical quantities stairs:

$$K_L - \text{length scale}, \; K_L = \frac{l_n}{l_m} \qquad (2.2)$$

$$K_m - \text{mass scale}, \; K_m = \frac{m_n}{m_m} \qquad (2.3)$$

$$K_t - \text{time scale}, \; K_t = \frac{t_n}{t_m}. \qquad (2.4)$$

$$K_v - \text{for speed} \quad K_v = \frac{v_n}{v_m} = \frac{\frac{l_n}{t_n}}{\frac{l_m}{t_m}} = \frac{K_L}{K_t} \qquad (2.5)$$

$$K_a - \text{for acceleration}, \; K_a = \frac{K_L}{K_t^2} \qquad (2.6)$$

$$K_F \text{ – for forces, } K_F = \frac{m_n \cdot a_n}{m_m \cdot a_m} = K_m \cdot \frac{K_L}{K_t^2} \tag{2.7}$$

where:

n – the development shows that it is a natural phenomenon;
m – indicates a similar phenomenon in the laboratory.

3. Numerical done and results

Functional dimensions which fit installation are [12]:

- Piston diameter (Dp) n = 0.6 m;
- Actual race (S) n = 6 m;

Hydraulic Linear Motor (MHL) functional dimensions which fit the model of sepsis are reduced:

- Piston diameter (Dp) m = 0.105 m;
- Actual race (S) m = 1.6 m;

Applying relations (2.1 to 2.6) examined the particular case are obtained:

$$K_L = \frac{(D_p)_n}{(D_p)_m} = \frac{0,6}{0,105} = 5,71 \tag{2.8}$$

$$K_t = \frac{t_n}{t_m} = \sqrt{K_L} = \sqrt{5,71} = 2,39 \tag{2.9}$$

$$K_v = \frac{K_L}{K_t} = \frac{5,71}{2,39} = 2,39 \tag{2.10}$$

$$K_v = \frac{K_L}{K_t^2} = \frac{5,71}{(2,39)^2} = 1 \tag{2.11}$$

$$K_F = K_m \cdot K_L \cdot K_t^{-2} = 32,62 \tag{2.12}$$

To take into account how closely the special phenomena that occur at high pressure, pressure scale should be:

$$K_p = \frac{(p)_n}{(p)_m} = 1 = K_m \cdot K_a \cdot K_L^{-2} = K_m \cdot \frac{1}{K_L \cdot K_t^2} \tag{2.13}$$

$$K_m = K_L \cdot K_t^2 = 5,71 \cdot 2,39^2 = 32,62 \tag{2.14}$$

Table 3.1. **Main size of one's values**

The main plant sizes from	Real	Model
Maximum dynamic force	9 MN	275.9 kN
Static dynamic force	11 MN	-
Maximum lowering speed	0.16 m/s	0.067 m/s
Maximum lifting speed	0.08 m/s	0.033 m/s

We can draw the following conclusion: the similarity is not fully realized, it is a partial similarity. To the extent that we see a similarity completely or partially, to check the main criteria of similarity [7].

Table 3.2. **Main criteria of similarity values**

No.	The criteria of similarity	Relationship definition	Value of real situation	Value model
1	Criterion Reynolds	$\mathrm{Re} = \frac{v \cdot l}{\nu}$	6400	469
2	Criterion Froude	$Fr = \frac{v^2}{L \cdot g}$	$4.349 \cdot 10^{-3}$	$4.35 \cdot 10^{-3}$
3	Criterion Strouhal	$Sh = \frac{v \cdot T}{L}$	1.94	3.82
4	Criterion Newton	$\mathrm{Ne} = \frac{\mathrm{F}}{\rho \cdot \mathrm{v}^2 \cdot \mathrm{l}^2}$	$125.2 \cdot 10^3$	$714 \cdot 10^3$

3.1. Determining the complex stress and displacement

Stand for the study of the behavior under complex dynamic system unconventional maneuver, is actually faithful copy by reducing size and mass scale of the actual installation. Installation structure is a spacious building trusses, welded and profile and is provided with vertical self-running rolls mobile platform during lifting and descent [13].

Dimensional and geometric configuration and materials used to scaling follows closely the conditions of the actual dimensions as in the case of SGR. Mobile platform is a fully executed construction of the board. Mobile platform is a welded construction and machining[4].

Setting loads

To reduce the volume of input required on nodes, bars and shares, using the concept of MODEL. This model consists of a mobile platform and structure guide reagent (figure 3.1) [5]:

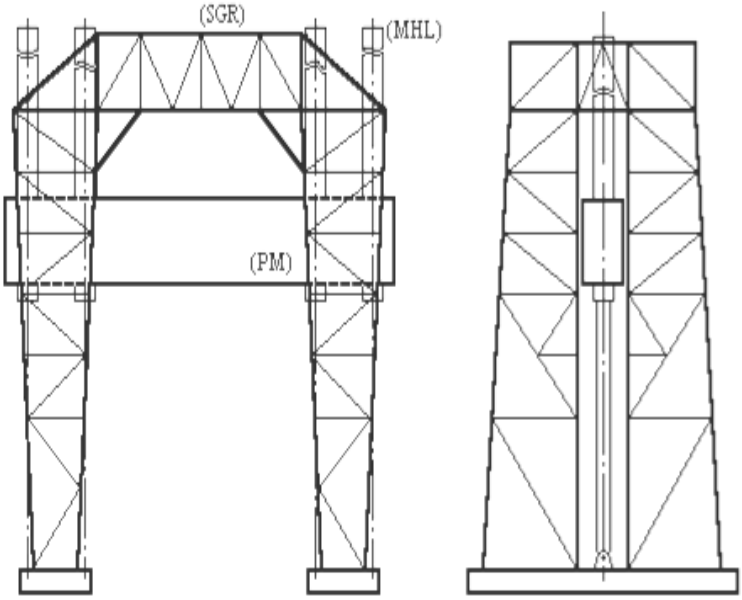

Figure 3.1. The model for unconventional rig

PM relies on the mobile platform MHL, which articulated the basic rods. This set is a mechanism characterized by two degrees of freedom: vertical displacement and rotation of the joint plan. SG allows sliding vertically (towards the movement PM) and suppress joint rotation axis, opposing forces and moments of this trend of couples reaction forces (reactive structure) [14].

In real operating conditions, the structure of reactive guidance, act as a multitude of factors: the weight of the elements, wind, additional forces due to mounting errors and displacements MHL desync appearance.

Designation and exceptional fundamental groups charge is made by applying the limit states method, the main criterion that governs these regulations it is the duration of action of metal constructions, which are divided accordingly [8],[11]:

Fundamental groups:

$$\sum_i n_i P_i + \sum_i n_i C_i + n_g \cdot \sum_i n_i V_i \qquad (3.1)$$

Exceptional groups:

$$\sum_i P_i + \sum_i C_i + n_g' \cdot \sum_i V_i + E_1 \qquad (3.2)$$

Constant load P – if SGR is resulting from the weight of the items (to be calculated with a subroutine program for each component). The burden of long term long-term C - for eleven days SGR is the resulting displacements of the mobile elements of the MHL and assembly errors. Because the literature is not known a method for calculating forces due to desync, will be further addressed this issue. Suitable for attaching the MHL scheme to PM(figure 3.2), the calculation results in two variants:

a) introduction of equivalent efforts desync motion

b) introducing equivalent desync shifting movement.

Variant a consider possible values of motion-desync MHL, evidenced by different values of the angle *S* the angle *b*): leading by following Δ, race differences are obtained α backward-compatibility geometric displacements, the emergence of additional efforts taken by the SG (*figure a*):

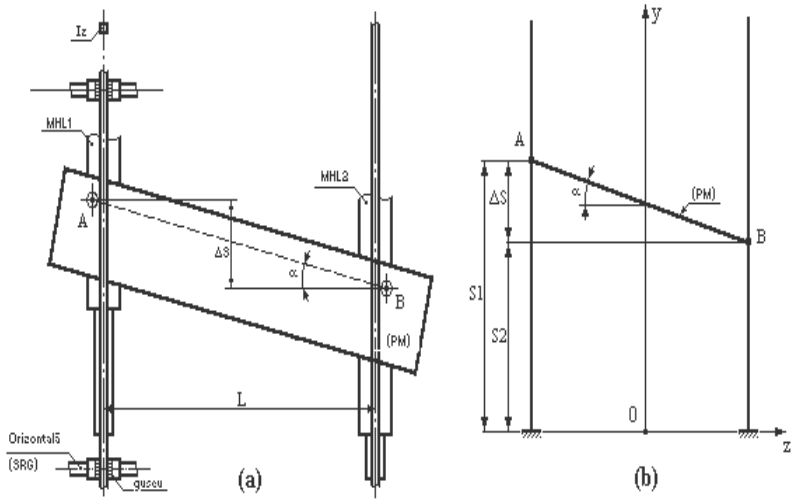

Figure 3.2. Functional schema of the PM trapping MHL

Considering the PM compared with infinite stiffness and rigidity of the SGR calculation scheme in figure 3.3, resulting SAGE in *xa* tread deformation of the structure under the effect desync, the following expression:

$$\frac{1}{2}\cdot x = \frac{L}{\cos\alpha} - L = L\cdot\left(\frac{1}{\cos\alpha} - 1\right) \tag{3.3}$$

$$X = 2\,x \tag{3.4}$$

where:

x – represents a single strain of the structure corresponding reactive directions;

X – accumulated strain under the action brought by eleven days efforts MHL motion-SG.

Calculation of deflection under the effect of efforts put desynchronizes used by the calculation scheme. Thus, the angle with values between 0 and 3° (5 – 6°), is regarded upon the direction of arrow *x* axis *0x*. The phenomenon described above is analogous to the elastic deformation of the tread under a force concentrated at a point after the arrow x direction (figure 3.3):

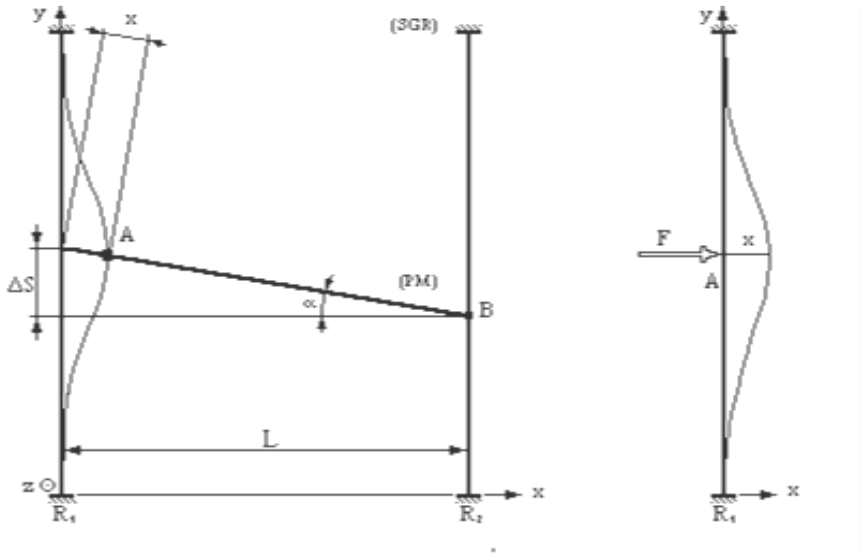

Figure 3.3. Scheme for calculating the force F, equivalent to the arrow x

The suitable elastic is known proportionality as:

$$F = kx \tag{3.5}$$

For a beam embedded at both ends of the arrow is the value:

$$x = \frac{F \cdot l^3}{2^6 \cdot 3 \cdot E \cdot I_z} \tag{3.6}$$

Relation 3.6 is valid in case the point where the force is at half concentrated beam an the supports do not suffer disposals elastic, a situation that is the worst case load. Resulting value of elastic constant *k*:

$$k = \frac{F}{x} = \frac{2^6 \cdot 3 \cdot E \cdot I_z}{l^3} \tag{3.7}$$

It is the moment of inertial the surface geometric section CR. The amount of force due to the end position desync displacements to obtain the general expression:

$$F_d = \frac{2^6 \cdot 3 \cdot E \cdot I_z}{l^3} \cdot \frac{L}{2} \cdot \left(\frac{1}{\cos\alpha} - 1 \right) \tag{3.8}$$

Another category of long-term temporary charge C, is the errors introduced the mounting forces). Force installation error that occurs in the MHL maximum, F max φ will be:

$$F\varphi_M = F_{max} \sin \varphi \tag{3.9}$$

FM is the maximum force of rod MHL.

Variant b properly angle produced by motion-MHL eleven days of PM, resulting deformities caused by the effect of PM directions inland.

Assuming acceptance of infinite rigidity of the construction PM in relation to SG, at the point of maximum lift height characteristic of PM, regarded as the worst case of manifestation of motion-MHL desync, because the arrow maximum product can be introduced into the calculation program translated by imposing a restriction disposals (elastic connections) for the node, the action point load properly, resulting in motion-MHL and eleven days after their course of action.

Force the action of short-term V-represented by the action of wind on PM and the SGR is calculated according to API:

$$F_{PM,MHL,SGR} = \beta \cdot C_t \cdot p \cdot A \tag{3.10}$$

Applying the limit states method to determine the charge groups is obtained:

After the 0x axis direction: the fundamental group of loads:

$$F_x = 1.2\ F_{max} + 1.3\ \ F_v \tag{3.11}$$

where:

load coefficients n1 = 1, n2 = 1.2, n3 = 1.3 were chosen according to [1];

F_x – is the result of all forces acting on the direction of the axis 0x, the point corresponding to the rate applied to PM peak.

After the axis 0y: P own weight, calculated automatically by a subroutine:

$$F_y = P \tag{3.12}$$

After the axis 0Z: desync forces resulting from:

$$F_Z = n_2 \cdot F_d = 1{,}2 \cdot F_d \tag{3.13}$$

These groups constitute the forces acting on SGR the load which will be subsequently determined by the complex state of stress and displacement using an electronic computer.

3.2. Determining the complex stresses and strains numerical simulation

The examples will be highlighted results when a scale model, made in the laboratory of the University of Ploiesti, where the real structure.

The model was discretized in 612 beam elements declared in the program, and 206 knots. These are highlighted in geometric configuration of the computer scheme (figure 3.4).

For variant *a* the calculation presented in the preceding paragraph, after running the program were determined with precision he tensions in the structure: axial force, shear after the two axes of the element bending, bending moments after the two axes of bending element and torque. He results show that the required elements of the SG are primarily those resulting from the tendency to take efforts to topple the SG, under the action of the fundamental group of loads.

It finds that large values of nodal displacements are recorded by nodes located at the top of the structure model, which is also a danger that rolls mobile platform to jump on the track (path). For variant b) calculation,

also presented in the preceding paragraph, after running the program were determined voltages equivalent unit on each element of the model structure, to various degrees of non-synchronization of the movement of PM MHL, translated by different values of the angle α for values of 1 and 6 and from grade level for each of the four legs.

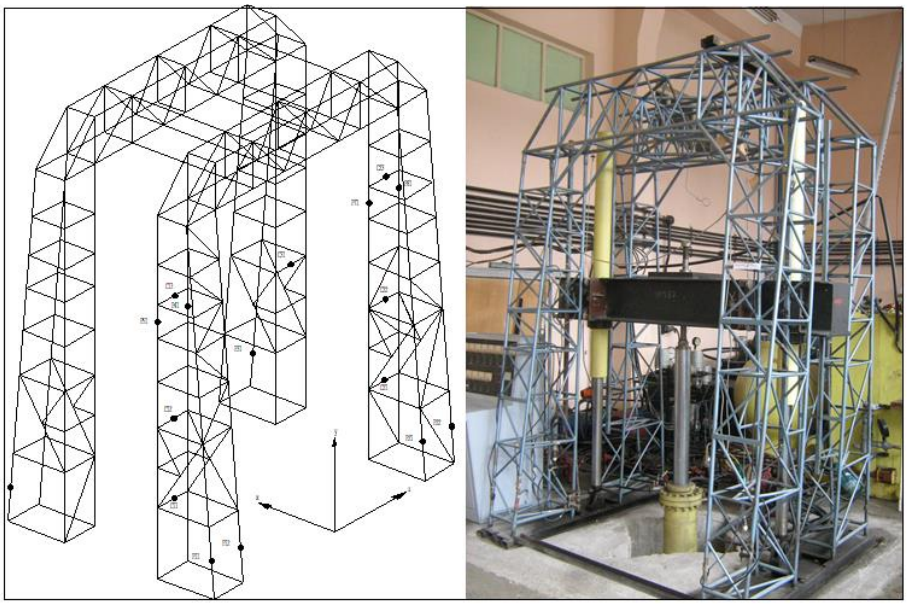

Figure 3.4. The computational model and physical model (SIMIL) it presents an overview of precise position measurement points

Shows the following:

– Equivalent unitary tensions high values occur in the elements located in the upper part of the SG corresponding maximum lifting height in the immediate vicinity of the PM pint (area) where there is movement on the structure under the action node inclination PM (table 3.3);

– Equivalent unitary elevated tension is developing the model structure for each leg of the tendency to topple over under the effect of SG desync motion

– The geometric parameter values greater than 3 and desync, equivalent uniform stress values on some items, exceeding the limit of endurance of the material is built model (endurance limit);

– Desync deformation structure under the effect of geometrical parameter increases exponentially with desynchronization.

Table 3.3. **Maximum depending on the angle "α" of inclination travers**

No		Node	Node						σ_{ech}	MPa				
	Beam	i	j		α=1		α=2		α=3		α=4		α=5	
				node i	node j	node i	node j	node i	node j	node i	node j	node i	node j	node i
1	443	17	165	1,619	1,489	5,90	2,97	13,01	54,28	23,04	8,9	35,86	13,33	51,53
2	444	165	166	2,38	2,35	5,62	2,92	11,0	3,86	18,61	5,18	28,31	6,87	40,17
3	445	166	167	1,38	0,474	6,66	0,012	15,43	-0,02	27,81	-0,04	43,62	-0,09	62,9
4	446	167	168	2,426	5,476	8,70	20,8	19,1	46,3	33,8	82,3	52,57	128	75,52
5	447	168	50	1,50	0,36	13,96	8,06	34,6	20,8	63,7	38,8	101	61,9	146
6	452	35	174	-2,54	13,14	-9,32	50,37	-20,5	112	-34,3	199	-56,7	310	-81,4
7	453	174	175	2,28	-0,39	9,54	-2,05	21,59	-4,7	38,61	-8,6	60,34	-13,6	86,9
8	454	175	176	1,12	4,74	1,77	11,46	3,25	22,5	5,34	38,3	8,01	58,4	11,28
9	455	176	177	3,93	4,69	10,28	20,5	20,80	46,69	35,36	83,7	54,6	131	77,8
10	456	177	178	-2,58	4,69	-10,8	19,7	-24,2	7,1	-43,1	79,9	-67,2	125	-96,6
11	448	169	170	0,33	1,98	1,50	7,63	3,44	17	6,19	30,2	9,65	47,1	13,9
12	449	170	171	-0,55	1,17	-0,54	2,44	-0,19	5,93	0,29	10,8	0,92	17,1	1,69
13	450	171	172	2,15	3,10	10,26	12,9	23,68	29,14	42,6	52,0	66,8	81,4	96,5
14	451	172	173	1,35	0,29	11,24	6,72	27,6	17,3	50,7	32,4	80,3	51,6	116
15	459	179	175	-2,54	13,14	-3,52	6,26	-7,32	13,53	-12,7	23,8	-19,5	36,9	-27,9
16	460	180	181	2,28	-0,39	5,15	-1,82	11,9	-2,87	21,6	-4,3	33,9	-62,6	48,9
17	461	181	182	0,99	3,37	2,93	16,09	6,15	37,1	10,7	66,9	16,5	105	23,6
18	462	182	183	2,85	0,92	2,01	12,2	48,7	30,93	89,2	57,3	44,3	43,9	204
19	497	184	185	1,94	0,99	7,29	6,07	16,08	15,05	9,41	42,8	94,6	134	63,7
20	498	185	186	4,51	4,78	15,7	21,0	34,49	47,9	60,9	86,0	218	-82,2	135

3.2. Determining the stresses and strains with tensometric measurements

Strain gauge were attached as an already known technology, using an appropriate adhesive, the structural elements that were to be investigated and which previously have been thoroughly cleaned of any trace of paint and oxides.

The relation between measurement sites and was conducted for carrier decks with wire screens, wireless-wired with a capacity of 60 pF/m. All sites related to active and passive strain gauge an (trade blind to compensate for temperature) were glued alloy and were protected.

As bearers signal amplifier currents were used to determine the dynamic elongation eight bridges (bridge strain gauge) and for continuous recording of two signals were used oscilloscopes, all devices equipped with the unfortunate UPP Department.

Looking at the joint request of the four legs of the SG by simultaneous tensometric measurements and, if we consider the accuracy of measurement equal, we can say that SG is applied evenly all the legs.

Regarding the evolutions values recorded system at the same measuring points for measuring variant to handle the lifting PM, lowering, respectively, shows the following (figure 3.5).

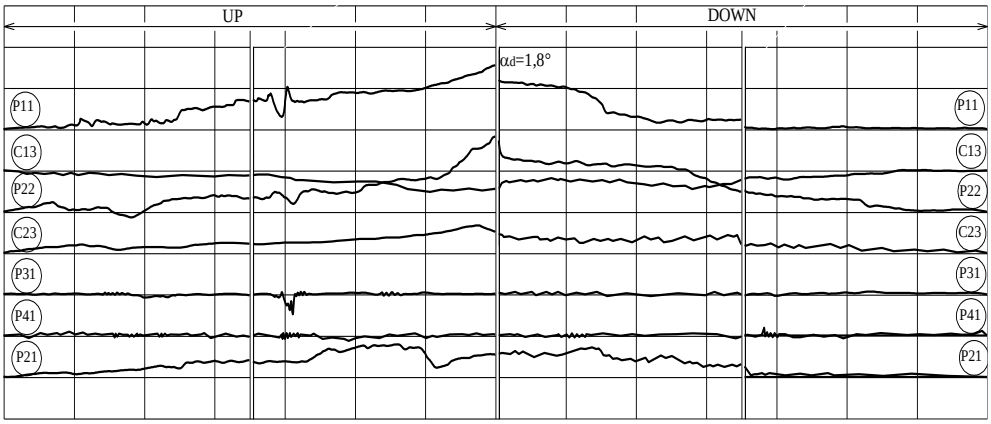

Figure 3.5. Some measurements for the structure SG with tensometric methods

To handle the lifting, loading structure is gradually becoming the maximum lifting height of the mobile platform, where eleven days is the maximum value (reached a value of the inclination of the platform in the foreground and $\alpha_{max} = 3^{o}$);

Lowering the maneuver, the structure is low gradually returning to the initial request, which is minimum when the mobile platform position is at the bottom;

Surgery for maneuver is accompanied by the phenomenon of vibration and other disturbances due to multiple shocks from four feet (four tracks), which can cause a completely random variation of effort (it is the fact that during the lifting or lowering, due to errors assembly, geometric asymmetries, mechanical or hydraulic, SG deformation during the maneuver.

The platform may not be in constant contact with the four rail tracks between them causing the failure, shock generators, for example a sudden discharge of the burden passed to one way of running appears as a sudden charge of its counterparts in the plane in which movement occurred PM.

To verify the theoretical research has been conducted under the effect of displacement measurements on request via the load, to determine the actual effects that occur.

For model with four legs and have chosen the following elements of the metallic structure for the measurement: (SG's rool beam and Corner pillars of legs);

Very important points of a lattice construction SG (results of the running computer program), they appear maximum equivalent stress of σ_{ech}.

The way in which these points were chosen to measure aimed at simultaneous coverage of the various requests in order to be able to analyze the tensions and, in particular, variation processes.

Also, the determination of strains was included in the program for measuring and recording the speed of the PM during the lifting operation.

Measurement of PM race lift during operation is indicated by means of potentiometers stand with particularity to run a maximum of 10 rotations in a voltage range from 0-5V.

Suitable lifting travel SM = 1.6 m fitted VMS potentiometer shaft run up to eight full rotations, which means a complete record of flight MS.

Mounted installation is composed of a thin steel cable which is fixed to the bottom of one leg of the SG and, respectively, at the top of the same leg, while last being over a roll and secured with metal shaft potentiometers which is fixed the PM. During displacement PM, lifting or lowering potentiometer system roll is enabled, because roller rolls over the wire stretched without slipping.

To request the lifting tower load, speed is important during the start (time to maximum peak demand).

According to the simplification proposed by the author to assess the results of measurement that will define the average speed during the active stroke.

4. Conclusions

As demonstrated by measurements on some records, the errors are greater than the allowable 8 %.

The phenomenon investigated is very complex and would have required a very large number of brands to increase the accuracy and amount of initial information.

In conclusion, the application due non synchronization SG movement almost permanently MHL has a character and must be included in the fundamental group of towers in charge of long term category temporary duties as a State whose application is given the maximum permissible value of desync.

This value occurs at maximum lift height of the PM and has given maximum value limits of the method adopted to drive SMN. Here then, a bidirectional link between the SG and the constructive design of SAH functional.

Specifically, research shows that the theoretical values of $\alpha_{Max} = 4.5$ and appear desync $\sigma_{ech} > \sigma_a$ of breaking and SG, So the synchronization

method used in the design must ensure MHL and SMN between limits, so the difference in travel to the end of the race do not bend more than 4.5º for PM.

For the second version of the plan measurement, developed to study the effect of lifting speed on the state of complex stress and displacement of the SG, measurements were made at average speeds, different in both lifting and descent, these values belong to interval 0.004 speed 0.017 m /s.

The conclusions from experimental measurements are as follows:

a) PM shift with a certain speed produces an increase in requests with greater speed maneuver as the increase.

b) Maximum demand occurs in the opening half that movement occurs because the rigidity of running the point and direction after displacement is minimal.

Finally, one can say that experimental research carried out has achieved its main objectives, providing a real picture of the phenomenon and a confirmation of analytical calculations and computer programs used mostly qualitative, quantitative aspect can be improved by means of statistical processing or outfit made with recording equipment and measure performance.

R E F E R E N C E S

[1] *Abrahamsen E., Reid D.* (2007) "*Improved well construction enabled by next generation top drive casing running and drilling tools"*, Weatherford Intl. Inc, SPE/IADC Drilling Conference, 20–22 February 2007, Amsterdam, The Netherlands.

[2] *Avram L.* (1995) „Guidance for Determining some Thermo- dynamic Variables during the Process of Well Cementing (with special references to wells with large diametre)", The Petroleum–Gas University of Ploiesti

[3] *Avram, L. Stan, M.* Study concerning the use of terrestrial experience in the domain of trial boring during the well water drilling on the Mars surface, Buletinul Universitatii Petrol-Gaze din Ploiesti, No 1/2010

[4] *Fraser C., Hitec Products Drilling; G. White, SPE, Rowan Drilling; and E. DePeuter* "LeTourneau Technologies" SPE/IADC Drilling Conference and Exhibition, 17-19 March 2009, Amsterdam, The Netherlands

[5] *Miguel Belarde, Shell Canada and Ola Vestavik* "Reelwell, Offshore Europe", 6-8 September 2011, Aberdeen, UK.

[6] *Martin Hofschröer, Bentec GmbH Drilling & Oilfield Systems, SPE/IADC* "Middle East Drilling Technology" Conference and Exhibition, 20-22 October 2003, Abu Dhabi, United Arab Emirates.

[7] Niculescu, Ș., Tehnologia Forării Sondelor, Editura Universității Ptrol – Gaze din Ploiești, 2000.

[8] *Stan, M*., Utilaj petrolier, Editura Universității Petrol - Gaze din Ploiești, 2010.

[9] Săvulescu, P., Utilaj petrolier for foraj-extracție, Editura Universităţi Petrol - Gaze din Ploiești, 2015.

[10] *Stan, M.* Estimarea fiabilităţii instalaţiilor de foraj utilizând modele matematice de structură, , Buletinul Universitătii Petrol – Gaze din Ploiesti, Nr.2/2005

[11] *Stan, M*. Metode avansate de proiectare a utilajului petrolier (ediţia a ii-a revizuită şi adaugită), Editura Universitatii Petrol-Gaze din Ploiesti, 2011.

[12] *STAN Marius , Mihail MINESCU,, Niculae-Napoleon ANTONESCU, Alexandru STAN* Vibration analysis in the process of operation of installations and machines from the oil industry, Vol. 6, Issue 3, pp. 94-126, DOI: 10.37410/EMERG.2020.3.09

[13] ***Composite Catalog of Oil Field Equipment & Services, http://books.google.ro/books/about/The_Composite_catalog_of_oil_field_equip.html

[14] *** Drilling rigs, http://en.wikipedia.org/wiki/Drilling_rig